Hindawi
Journal of Advanced Transportation
Volume 2023, Article ID 3633058, 11 pages
https://doi.org/10.1155/2023/3633058

Research Article

Road Adhesion Coefficient Estimation Based on Vehicle-Road Coordination and Deep Learning

Chunjie Li,[1,2,3] **Pan Liu**,[1] **Zhenlong Xie**,[2,3] **Zhibin Li**,[1] **and Huan Huan**[3]

[1]*School of Transportation, Southeast University, Nanjing 211189, China*
[2]*Hebei Provincial Communications Planning and Design Institute, Shijiazhuang 050011, China*
[3]*Vehicle-Road-Cloud-Network (Hebei) Industrial Research Center, Shijiazhuang 050011, China*

Correspondence should be addressed to Pan Liu; liupan@seu.edu.cn

Received 1 September 2022; Revised 31 October 2022; Accepted 13 April 2023; Published 5 May 2023

Academic Editor: Wen Liu

Accurate estimation of the road adhesion coefficient can help drivers and vehicles perceive changes in road state effectively, reducing the occurrence of traffic crashes accordingly. Therefore, this paper proposes a road adhesion coefficient estimation method based on vehicle-road coordination and deep learning. Firstly, a vehicle-based data feedback system combined with a vehicle-road network cloud is introduced, and CarSim simulation is used to expand the data set and train the model effectively. Then, the dynamic analysis of the whole vehicle is carried out, and the vehicle operation data related to the adhesion coefficient are obtained as the input of the estimation model. Then a combined model of road adhesion coefficient estimation based on self-attention (SA), convolutional neural network (CNN), and long short-term memory (LSTM) is established, to reduce the instability of the prediction, *Q*-learning is used to optimize the weight of the model. Finally, the model is verified by the simulation data and the actual vehicle-based data. The results show that the vehicle-based data feedback system combined with the vehicle-road network Ccloud is effective, and compared with other commonly used model, the estimation model proposed in this paper can effectively predict the road adhesion coefficient.

1. Introduction

With the growth of car ownership and the increase in people's travel frequency, the incidence of traffic accidents also grows. The reduction of the road friction coefficient caused by weather and other environmental conditions is an important factor in inducing these accidents. Especially in conditions with poor road adhesion and abrupt changes, the driver's ability to judge road safety is weakened, which is very easy to result in the vehicle's crash and sideslip [1]. In order to reduce the occurrence of crashes, cooperative vehicle infrastructure system has become an inevitable trend. The effective estimation of the road adhesion coefficient is helpful for the system to change the control strategy in due course and reduce the occurrence of accidents [2].

Scholars around the world have carried out many research studies in the field of adhesion coefficient estimation for decades and achieved a series of results. Generally, the methods can be divided into cause-based and effect-based.

The cause-based methods predict the adhesion coefficient by collecting road surface information and combining previous experience [3]. This method can identify the road adhesion coefficient in real time under any working environment, but it needs to add additional sensors and other facilities, with high cost and high requirements for the installation position and durability of the sensors. Morii et al. [4] emit a high-power laser on the road and estimate the road condition according to the feedback information. Ko et al. [5] proposed to directly measure road materials and surface roughness through optical sensors so as to judge road type and predict adhesion coefficient. Hong et al. [6] proposed using acoustic sensors to measure the noise of tire to identify the road adhesion coefficient. However, the noise is easily affected by the environment, and the noise signal is

complex, so this method is difficult to estimate accurately. Paulo and Coelho [7] used a combination of Bayesian analysis and a neural network to classify the road through the sound signal of the tire contacting the ground and the macrotexture information collected by the contour curve instrument.

The development and application of connected automatic vehicles and cooperative vehicle infrastructure system can create an effective channel for data collection between driving environment and vehicles, and these data can be used to estimate the road adhesion coefficient. The effect-based estimation method is used to estimate the road adhesion coefficient by detecting the motion response of the vehicle body and wheels caused by the road condition. Many studies have used vehicle dynamics models or various tire road models. Such methods generally do not need to add additional sensors, and do not require serious working environment; so they have attracted dramatic attention. Enisz et al. [8] proposed to estimate the maximum and instantaneous value of the tire road adhesion coefficient based on magic tire formula and the extended Kalman filter algorithm. Ma et al. [9] proposed to estimate the sideslip angle of the tire through the unscented Kalman filter, and then formulated the identification rules of the adhesion coefficient in combination with the positive torque of a single wheel. Peng et al. [10] estimated the tire force by designing a filter observer, and then designed a nonlinear observer to estimate the adhesion coefficient at the same time. Ping et al. [11] proposed an adaptive road adhesion coefficient estimation scheme using weighted attenuation memory unscented Kalman filter to improve the accuracy. Hu et al. [12] used the extended Kalman filter to estimate the lateral speed of the vehicle, and then successively designed two traceless Kalman filters to estimate the tire force and adhesion coefficient, respectively, reducing the computational burden. Shao et al. [13] proposed an innovative optimization-based framework for road adhesion estimation. This framework implements a grid search method for solving nonconvex optimization problems, which can estimate μ Max and sideslip angle accurately in real time without making good initial guesses on nonconvex optimization.

The traditional tire road model relies on the professional testing of tires to collect optical, acoustic, or other physical signals. After changing the tire or vehicle parameters, its characteristic curve will be changed accordingly. With the development of artificial intelligence, deep learning and reinforcement learning are gradually being applied to the field of traffic control and optimization [14]. Therefore, many scholars have applied the deep learning model to the estimation of road adhesion coefficients in recent years, which has gradually become a research hotspot [15]. Sun et al. [16] proposed an improved algorithm based on the forgetting Kalman filter by adding a forgetting factor to estimate the slope of the curve under low slip rates. Li et al. [17] proposed a road friction coefficient identification method based on support vector machine (SVM), which can effectively identify the road adhesion coefficient in the steering process under different road conditions. Based on the analysis of vehicle dynamics, Kim et al. [18] used the slip ratio, normalized longitudinal force, and longitudinal acceleration as inputs and used SVM and DNN models to predict the friction coefficient between tire and road. The results showed that DNN has higher accuracy. Ribeiro et al. [19] used the data of vehicle speed, acceleration, yaw angle, and other data combined with a time delay neural network (TDNN) to estimate the road adhesion coefficient and achieved good results. Choi et al. [20] proposed to combine the longitudinal and transverse tire brush models, and through the linear recursive least squares method, it has a good recognition effect on the road. Eldar et al. [21] proposed using video data to estimate the friction coefficient and improving vehicle dynamics control through the anti-brake system.

To sum up, in the field of road adhesion coefficient estimation, the cause-based method has high requirements for equipment. The empirical model or tire-road model in the effect-based method lacks portability, and the characteristic curve is easy to change. In the aspect of machine learning, scholars often use a single deep neural network (DNN) model as the main deep learning model at present, and there is still room for improvement in the ability to process nonlinear data and increase prediction accuracy only by relying on the fully connected neural network. In order to fully use the vehicle operation data to serve the vehicles and traffic in real time, it has gradually become a hot direction to integrate and calculate the data of vehicle operation and establish an intelligent connected system by using cutting-edge information and communication technologies such as cloud computing, 5G, and the Internet of Things.

Therefore, this paper proposes a new method to estimate the road adhesion coefficient based on the vehicle-based data feedback system combined with the vehicle-road network cloud. Firstly, the system is introduced, and to expand the data set and facilitate model training, vehicle operation data under different road conditions are collected through CarSim simulation in Section 2. Then, the dynamics of the whole vehicle is analyzed to determine the input vector of the model in Section 3. Section 4 introduces a combined model of deep learning. SA-CNN-LSTM is built to predict the adhesion coefficient. Aiming at the problem that the predicted value of the model exceeds the range of common sense, reinforcement learning is proposed to improve the combined model of deep learning. The simulation data and the collected real vehicle-based data are used to verify the model in Section 5. Section 6 concludes with the contributions of this research.

2. Data Collection

2.1. Vehicle-Based Data Feedback System Combined with Vehicle-Road Network Cloud. This paper uses the vehicle-based data feedback system that incorporates the vehicle, road, network, and cloud in Hebei Province, China. The vehicle-based data feedback system establishes a data exchange and integrated system with the traditional network inside the vehicle (CAN, Lin, vehicle-based Ethernet, etc.)

and the wireless communication network in the wide area (4G/5G cellular, C-V2X) to connect the vehicle operation data with the traffic management information. It aims to establish a new collaboration system between the vehicle operation system and the road that uses vehicle data as microscopic input, uses macroscopic data on integrated road traffic, and provides services for individual vehicles as a way of traffic management and applications. The composition of the vehicle-based data feedback system is shown in Figure 1. The overall technical architecture consists of cloud platforms, intelligent infrastructure on the roadside, and intelligent vehicle terminals.

In the vehicle-based data feedback system, the intelligent terminal of the vehicle can sense the vehicle information in real time, obtain the vehicle operation data, and transmit the data to the cloud computing platform. The intelligent infrastructure of the road section can monitor the road status in real time, realize the road digitization, and transmit the road traffic information to the cloud platform. The cloud platform completes the collaborative perception decision of vehicles and realizes the collaborative control with road sections through calculation.

The characteristics and core technologies of the vehicle-based data feedback system are different from traditional collaboration between vehicle and road in three ways. Firstly, it provides an integrated technological system with the networks for vehicles, roads, and third-party data standards. Secondly, it establishes a communication connection between networks in vehicles and the traffic environment of the road, collects vehicles' operation data, transports them to the cloud, and calculates the data from the roadside and cloud. Thirdly, it makes full use of cloud computing platform technology to construct fundamental data formation based on vehicle-based feedback. It also does data mining on the basis of a data warehouse with multiple sources and purposes. The vehicle-based data feedback system is an application system that is driven by a centralized platform, which is based on a uniform fundamental data standard. It has a high degree of scalability in terms of the integration of vehicle, road, network, and cloud.

The vehicle-based data system can provide real-time vehicle operation data through intelligent vehicle terminal, as shown in Figure 2. The collected data includes vehicle number, longitude, latitude, speed, lateral acceleration, steering angle, longitudinal acceleration, yaw rate, wheel angular speed, operating mode of ACC (adaptive cruise control), status of ABS (antilock braking system), and other fields. The data are stored in the cloud platform and the time interval of data is 100 ms.

2.2. Simulation Data. Due to the limitations of sensors and other factors, the vehicle-based system cannot obtain the value of the road adhesion coefficient in real time. In the process of establishing the estimation model of travel road adhesion coefficient and evaluating the model, it is necessary to have the vehicle operation data under the condition of a known road adhesion coefficient. The process of using the traditional single-wheel lateral force test vehicle is complex, and it will affect the normal travel of other people. The cost of collecting vehicle operation data through the system is also high. Therefore, this paper expands the data set through Carsim simulationand uses the simulation data to train the deep learning model, which will be introduced in Section 4.

In CarSim simulation, this paper constructs two kinds of travel roads, straight and circular, with the speed set at 0–120 km/h, accelerating first and then decelerating. In order to cover more different scenarios, the adhesion coefficient of road is divided into two categories: fixed adhesion coefficient and variable adhesion coefficient. There are three kinds of roads with fixed adhesion coefficient: low adhesion coefficient roads with adhesion coefficient of 0.2, medium adhesion coefficient roads with adhesion coefficient of 0.5, and high adhesion coefficient roads with adhesion coefficient of 0.8. There are two types of roads with variable adhesion coefficient: roads with increasing adhesion coefficient (road adhesion coefficient is divided into four sections: 0.1, 0.3, 0.6, and 0.9), and roads with decreasing adhesion coefficient (road adhesion coefficient is divided into four sections: 0.9, 0.6, 0.3, and 0.1). Some parameters of the vehicle model simulated by CarSim are shown in Table 1. The simulation data are collected once every 100 ms, and the simulation time of each experiment is 40 seconds.

3. Vehicle Dynamics Analysis

3.1. Force Analysis of the Whole Vehicle. Firstly, the stress of the whole vehicle and each tire of the vehicle should be analyzed. The transverse and longitudinal stresses of the whole vehicle are as follows:

$$\begin{aligned} ma_x &= (F_{x1} + F_{x2})\cos\delta - (F_{y1} + F_{y2})\sin\delta + F_{x3} + F_{x4}, \\ ma_y &= (F_{x1} + F_{x2})\sin\delta + (F_{y1} + F_{y2})\cos\delta + F_{y3} + F_{y4}, \end{aligned} \tag{1}$$

where m represents the mass of the whole vehicle; a_x and a_y represent the lateral and longitudinal acceleration of the vehicle; δ represents the angle of the front wheel of the vehicle; F_{x1}, F_{x2}, F_{x3}, and F_{x4}, respectively represent the lateral forces of the left front wheel, the right front wheel, the

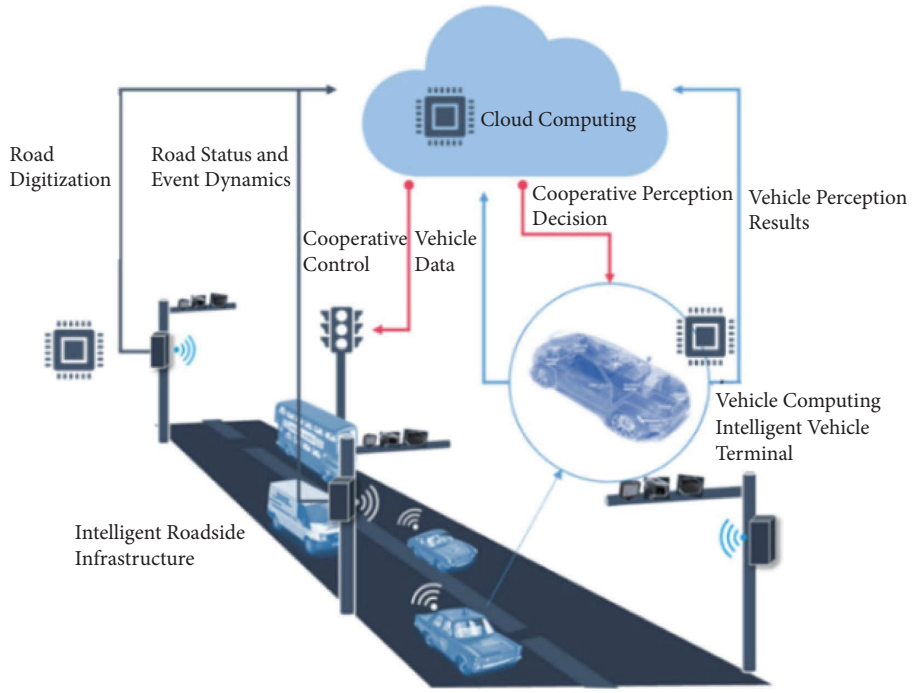

Figure 1: Structure of the data feedback system.

Figure 2: Vehicle collecting data.

Table 1: Vehicle model parameters of CarSim.

Vehicle condition	Value
Vehicle quality	2335 kg
Vehicle length ∗ width ∗ height	5035 ∗ 1989 ∗ 1778 mm
Tire diameter	20 inches
Vehicle wheelbase	3008 mm
Minimum ground clearance	190 mm

left rear wheel, and the right rear wheel of the vehicle; F_{y1} andF_{y2} represent the lateral force of the left front wheel and the left rear wheel of the vehicle, respectively.

The vertical load calculation formula of each tire is

$$\begin{aligned}
F_{z1} &= \frac{(\mathrm{mgl}_r)}{(2(l_f+l_r))} - \frac{(\mathrm{ma}_x h)}{(2(l_f+l_r))} - \frac{(\mathrm{ma}_y l_r h)}{(2(l_f+l_r)d_r)} - \left(\frac{K_1\chi}{2d_f}\right),\\
F_{z2} &= \frac{(\mathrm{mgl}_r)}{(2(l_f+l_r))} - \frac{(\mathrm{ma}_x h)}{(2(l_f+l_r))} + \frac{(\mathrm{ma}_y l_r h)}{(2(l_f+l_r)d_r)} + \left(\frac{K_1\chi}{2d_f}\right),\\
F_{z3} &= \frac{(\mathrm{mgl}_f)}{(2(l_f+l_r))} + \frac{(\mathrm{ma}_x h)}{(2(l_f+l_r))} - \frac{(\mathrm{ma}_y l_f h)}{(2(l_f+l_r)d_r)} - \left(\frac{K_2\chi}{2d_r}\right),\\
F_{z4} &= \frac{(\mathrm{mgl}_f)}{(2(l_f+l_r))} + \frac{(\mathrm{ma}_x h)}{(2(l_f+l_r))} + \frac{(\mathrm{ma}_y l_f h)}{(2(l_f+l_r)d_r)} + \left(\frac{K_2\chi}{2d_r}\right),
\end{aligned} \tag{2}$$

where F_{z1}, F_{z2}, F_{z3}, and F_{z4} represent the vertical force of the four tires; g represents the gravitational acceleration; l_f and l_r represent the distance from the center of mass to the front axle and the rear axle, respectively; d_r and d_f represent the track width of the front wheel and the rear wheel, respectively; K_1 and K_2 represent the front axle roll stiffness and the rear axle roll stiffness, respectively; and χ indicates the body roll angle.

3.2. Tire Model. The Dugoff tire model [22] requires few parameters and has simple expression. Therefore, this paper selects the Dugoff model to express tire characteristics. The specific formula is as follows:

$$F_{\mathrm{yi}} = \left(\frac{C_y \tan\alpha_i}{(1+\alpha_i)}\right) f(\lambda_i), \tag{3}$$

$$F_{\mathrm{xi}} = \frac{C_x \sigma_i}{(1+\sigma_i)} f(\lambda_i), \tag{4}$$

$$f(\lambda_i) = \begin{cases} 1, & \lambda_i \le 1, \\ (2-\lambda_i)\lambda_i, & \lambda_i > 1, \end{cases} \tag{5}$$

$$\sigma_i = \frac{\mathrm{Rw}_i - v_i}{\max(\mathrm{Rw}_i, v_i)}, \tag{6}$$

$$\lambda_i = \frac{\mu F_{\mathrm{zi}}(1+\sigma_i)}{\sqrt{(C_x\sigma_i)^2 + (C_y \tan\alpha_i)^2}}, \tag{7}$$

where C_y and C_x represent the longitudinal stiffness and lateral stiffness of the tire, respectively; σ_i represents the longitudinal slip ratio; α_i represents the sideslip angle of the tire; μ represents the adhesion coefficient of road; $\lambda_i > 1$ indicates that the wheel is in the linear state region; $\lambda_i \le 1$ indicates that the wheel is in the nonlinear state region; v_i represents the center speed of the tire; R represents the tire radius; w_i represents the wheel angular speed; and $i\,(i = 1, 2, 3, 4)$ represents the left front wheel, the right front wheel, the left rear wheel, and the right rear wheel, respectively.

The formula of the tire sideslip angle is

$$\begin{aligned}
\alpha_1 &= \delta - \arctan\left(\frac{v_y + l_f w_r}{v_x - (b_f/2)w_r}\right),\\
\alpha_2 &= \delta - \arctan\left(\frac{v_y + l_f w_r}{v_x + (b_f/2)w_r}\right),\\
\alpha_3 &= -\arctan\left(\frac{v_y - l_r w_r}{v_x - (b_r/2)w_r}\right),\\
\alpha_4 &= -\arctan\left(\frac{v_y - l_r w_r}{v_x + (b_r/2)w_r}\right).
\end{aligned} \tag{8}$$

3.3. Input of Neural Network. By substituting the expressions of F_x and F_y of the tire model into the force analysis of the whole vehicle, the following can be obtained:

$$\begin{aligned}
\mathrm{ma}_{\mathrm{x}} &= \left(\left(\frac{C_x\alpha_1}{(1+\sigma_1)}\right)\cos\delta - \left(\frac{C_y\tan\alpha_1}{(1+\sigma_1)}\right)\sin\delta\right)(2-\lambda_1)\lambda_1\\
&\quad + \left(\left(\frac{C_x\alpha_2}{(1+\sigma_2)}\right)\cos\delta - \left(\frac{C_y\tan\alpha_2}{(1+\sigma_2)}\right)\sin\delta\right)(2-\lambda_2)\lambda_2\\
&\quad + \left(\frac{C_x\alpha_3}{(1+\sigma_3)}\right)(2-\lambda_3)\lambda_3\\
&\quad + \left(\frac{C_x\alpha_4}{(1+\sigma_4)}\right)(2-\lambda_4)\lambda_4.\\
\mathrm{ma}_y &= \left(\frac{C_x\alpha_1}{(1+\sigma_1)}\cos\delta + \frac{C_y\tan\alpha_1}{(1+\sigma_1)}\sin\delta\right) f(\lambda_1)\\
&\quad + \left(\frac{C_x\alpha_2}{(1+\sigma_2)}\cos\delta + \frac{C_y\tan\alpha_2}{(1+\sigma_2)}\sin\delta\right) f(\lambda_2)\\
&\quad + \frac{C_x\alpha_3}{(1+\sigma_3)} f(\lambda_3) + \frac{C_x\alpha_4}{(1+\sigma_4)} f(\lambda_4).
\end{aligned} \tag{9}$$

The expressions of $f(\lambda_i)$ and λ_i are shown in equations (5) and (7). Therefore, when the wheel is in the nonlinear state region, ma_x and ma_y can be regarded as a quadratic function of μ, and it can be concluded that the road adhesion coefficient is related to the longitudinal slip rate σ_i, tire sideslip angle α_i, front wheel angle of the vehicle δ, longitudinal acceleration a_x, and lateral acceleration a_y. When the wheel is in the linear state region, the road adhesion coefficient μ is related to the longitudinal slip rate σ_i and the tire side slip angle α_i, but the longitudinal slip rate and the tire side slip angle are difficult to measure in the actual vehicle operation. However, they can be obtained from the

vehicle speed and the tire angular speed. Therefore, the yaw rate, longitudinal speed, lateral speed, and angular speed of each wheel are taken as the inputs of the road adhesion coefficient prediction model.

4. The Estimation Model of the Road Adhesion Coefficient

The road adhesion coefficient estimation model established in this paper includes two parts: the combined deep learning prediction model and the reinforcement learning optimization model, as shown in Figure 3. Each model will be described in detail later.

The combined deep learning prediction model is composed of self-attention, CNN, and LSTM. There is a spatial correlation between vehicle speed, yaw angle, and wheel angular velocity at the same time. In the process of vehicle operation, there is temporal continuity between adjacent times. Previous studies have shown that the convolution operation of CNN has strong advantages in extracting spatial features of data [23]. Due to its long-term memory function, LSTM can effectively extract temporal features [24]. Therefore, the combination model built in this paper is based on CNN-LSTM [25]. In addition, since the advent of self-attention, it has been widely used in many fields and can mine the correlation between original data. Therefore, this paper adds a self-attention mechanism to the CNN-LSTM to help the model capture the relationship between vehicle operation data and road adhesion better. In order to improve the generalization ability of the model and make it learn more effective features from the limited data, K-fold cross-validation is used in the training process. Different parts of the original data are divided into a training set and a validation set many times.

During the training set prediction of the combined model, the predicted value of the adhesion coefficient may be greater than 1 or less than 0. The paper used the idea of reinforcement learning to solve this problem. Reinforcement learning methods emphasize how to act based on the environment to maximize the expected benefits, that is, how the agent can produce the behavior that can obtain the maximum benefits under the reward and punishment mechanisms given by the environment. In this paper, action refers to the weight and bias of the model, which are obtained through training, and output refers to the predicted value of the road adhesion coefficient by the model. The reward mechanism is set so the the predicted value of the adhesion coefficient is between 0 and 1. If the predicted value of the adhesion coefficient is less than 0 or greater than 1, a penalty will be given.

4.1. Self-Attention. Attention mechanism has gradually become the focus of research in recent years, and it is used to solve various problems [26]. The use of self-attention makes the model easier to capture long-distance interdependent features [27], which will directly connect any two features in the data.

$$\begin{aligned} Q &= W^q X^i, \\ K &= W^k X^i, \\ V &= W^v X^i, \\ \text{Attention}(Q, K, V) &= \text{softmax}\left(\frac{QK^T}{\sqrt{d_k}}\right)V, \end{aligned} \tag{10}$$

where X^i is the model input sequence matrix; W^q, W^k, and W^v represent the weight matrix; Q, K, and V represent the query vector, key vector, and value vector, respectively. d_k represents a dimension of a query vector and a key vector.

4.2. CNN. One-dimensional CNN has good performance in extracting spatial features of time series data [28]. To enhance the feature extraction ability of the model for nonlinear data [29], the CNN constructed in this paper includes two convolution layers and a pool layer.

The convolution layer uses the same kernel to traverse the input according to a fixed step size. At each position traversed, the convolution kernel and the neurons of the upper layer perform convolution operation. The operation formula is

$$y^{(i,j)} = w * x^{(i,j)}, \tag{11}$$

where w represents the weight of the convolution kernel, $x^{(i,j)}$ represents the convolution region with the start (i, j), and $y^{(i,j)}$ represents the result of convolution.

In order to reduce the number of parameters and avoid overfitting, this paper uses maximum pooling, that is, for each region of the feature, only the maximum value is retained.

4.3. LSTM. LSTM is an improved recurrent neural network (RNN). Its structure includes a group of interconnected recurrent networks [30]. Each network contains three units: input gate, output gate, and forgetting gate, which respectively correspond to the input sequence and the previous state. The model process is as follows:

$$\begin{aligned} f_t &= \sigma\left(W_f\left[h_{t-1}, x_t\right] + b_{\text{ft}}\right), \\ i_t &= \sigma\left(W_i\left[h_{t-1}, x_t\right] + b_i\right), \\ \widetilde{C}_t &= \tan\text{h}\left(W_C\left[h_{t-1}, x_t\right] + b_C\right), \\ C_t &= f_t C_{t-1} + i_t \widetilde{C}_t, \\ o_t &= \sigma\left(W_o\left[h_{t-1}, x_t\right] + b_o\right), \\ h_t &= o_t * \tan\text{h}\left(C_t\right), \end{aligned} \tag{12}$$

where f_t, i_t, and o_t represent the vector calculation function of forgetting gate, input gate, and output gate; $\widetilde{C}_t$ represents the candidate state information; σ represents the sigmoid function, W_f, W_i, W_c, and W_o represent the weight matrix; b_{ft}, b_i, b_c, and b_o represent the offset term; x_t represents the operation data of the vehicle at the time t; C_{t-1} represents the

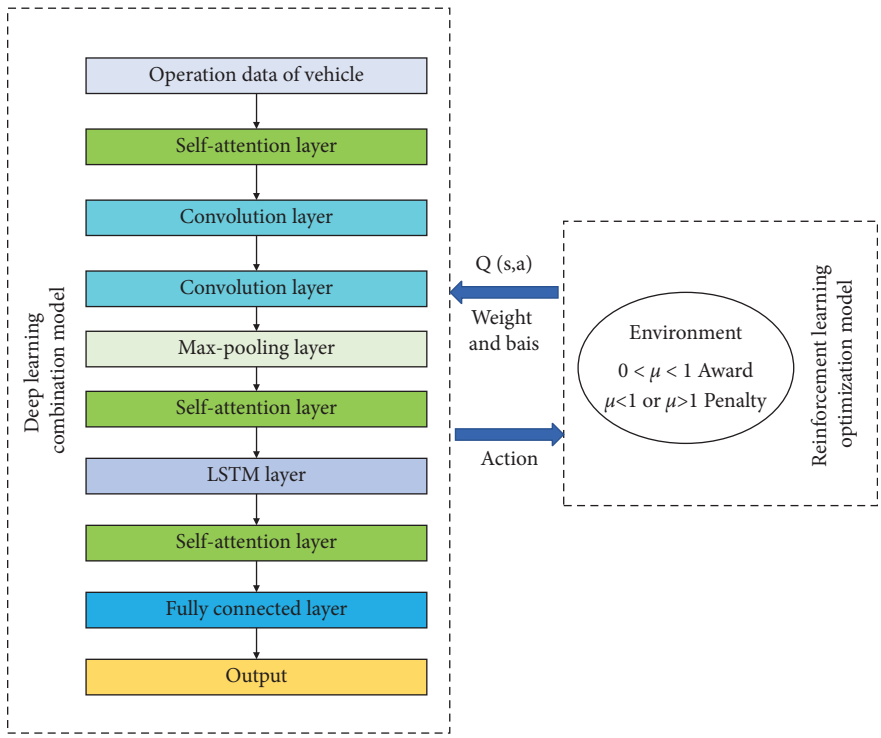

Figure 3: Structure of the adhesion coefficient estimation model.

memory of the previous time; h_t represents the LSTM output vector; and tanh represents the tanh function.

4.4. Q-Learning. In the field of reinforcement learning, Q-learning is one of the most widely used algorithms [31]. Its idea is to directly optimize an iteratively computed Q function, which represents the expectation of the return obtained by executing an action in a certain state and then executing it according to the optimal action sequence. The algorithm is widely used in traffic control and optimization. Through the Q-learning algorithm, the weight and bias terms of the combined deep learning model can be adjusted. By continuously giving punishment feedback, the road adhesion coefficient can be stabilized within the normal range, and the situation where the adhesion coefficient is less than 0 or greater than 1 is alleviated. According to Bellman's equations, the update formula of Q function is as follows [32]:

$$Q(s_t, a_t) \leftarrow Q(s_t, a_t) + \beta[r_{t+1} - Q(s_t, a_t) + \gamma \max Q(s_{t+1}, a_{t+1})], \tag{13}$$

where β represents the learning rate, γ represents the discount factor, and r_{t+1} represents the real-time reward obtained by taking action a_t in the state s_t. Select the largest $Q(s_{t+1}, a_{t+1})$ from the next state s_{t+1}. $Q(s_{t+1}, a_{t+1})$ value multiplied by decay γ. In addition, the true return value is the most realistic, and $Q(s_t, a_t)$ in the past Q table is used as the estimate.

5. Case Analysis

5.1. Simulation Data. The simulation data are divided into training set and test set by 4 : 1. DNN [18], CNN, and ConvLSTM are compared. The root mean square error (RMSE) and mean absolute error (MAE) are used to measure the prediction error. The formula is as follows:

$$\text{RMSE} = \sqrt{\frac{1}{n}\sum_{i=1}^{n}(p_i - y_i)^2}, \qquad \text{MAE} = \frac{1}{n}\sum_{i=1}^{n}|p_i - y_i|, \tag{14}$$

where p_i represents the predicted value of the model, y_i is the real value of the adhesion coefficient, and n represents the amount of data.

In each case, two experiments were conducted. The first experiment was used for model training, and the second experiment was used for model verification. When the road adhesion coefficient is stable, the real value of the simulation data of the second experiment is randomly selected and compared with the predicted value of each model. When the road adhesion coefficient changes, the real value near the sudden change point of the road adhesion coefficient in the second experiment is selected to compare with the predicted value of various models. The prediction results are shown in the following figure and table. The abscissa in the figure represents the sequence of selecting the display points, and

the ordinate represents the predicted value of the road surface adhesion coefficient.

Under the condition of low adhesion coefficient, the effect of each model is shown in Figure 4 and Table 2.

Under the condition of low adhesion coefficient road, compared with common models, the combined model proposed in this paper reduces RMSE by 29.41% and MAE by 33.3%. The improved combination model can further reduce 25% and 20% in the two indexes.

Under the condition of medium adhesion coefficient, the effect of each model is shown in Figure 5 and Table 3.

Under the condition of medium adhesion coefficient road, compared with common models, the combined model proposed in this paper reduces RMSE by 25.57% and MAE by 25%. The improved combination model can further reduce 20% and 22.2% in the two indexes.

Under the condition of high adhesion coefficient, the effect of each model is shown in Figure 6 and Table 4.

Under the condition of high adhesion coefficient road, compared with common models, the combined model proposed in this paper reduces RMSE by 27.78% and MAE by 25%. The improved combination model can further reduce 23.1% and 10% in the two indexes.

Under the condition of increasing adhesion coefficient, the effect of each model is shown in Figure 7 and Table 5.

Under the condition of increasing adhesion coefficient, compared with common models, the combined model proposed in this paper reduces RMSE by 19.23% and MAE by 22.2%. The improved combination model can further reduce 23.8% and 21.4% in the two indexes.

When the adhesion coefficient decreases, the effect of each model is shown in Figure 8 and Table 6.

Under the condition of increasing adhesion coefficient, compared with common models, the combined model proposed in this paper reduces RMSE by 8% and MAE by 21.1%. The improved combination model can further reduce 21.7% and 13.3% in the two indexes.

5.2. Real Vehicle-Based Data. In order to carry out the real vehicle test, the test vehicle and the cloud platform of the vehicle-based data feedback system are built. The test vehicle is equipped with an intelligent vehicle terminal. The built cloud platform can obtain the data of vehicle operation in real time, calculate the estimated adhesion coefficient, and record the results. A single-wheel transverse force coefficient test vehicle is selected for the comparative test. The vehicle has two test wheels, left and right, which can output the test data of the transverse force coefficient of the road under the wheel in wet conditions.

The real vehicle test is carried out on the forward and reverse roads of the 10 km expressway. The weather condition on the test day was fine. Because the friction coefficient estimation algorithm requires the vehicle to have accelerations, the test vehicle drives by accelerating first and then decelerating until the test section is completed.

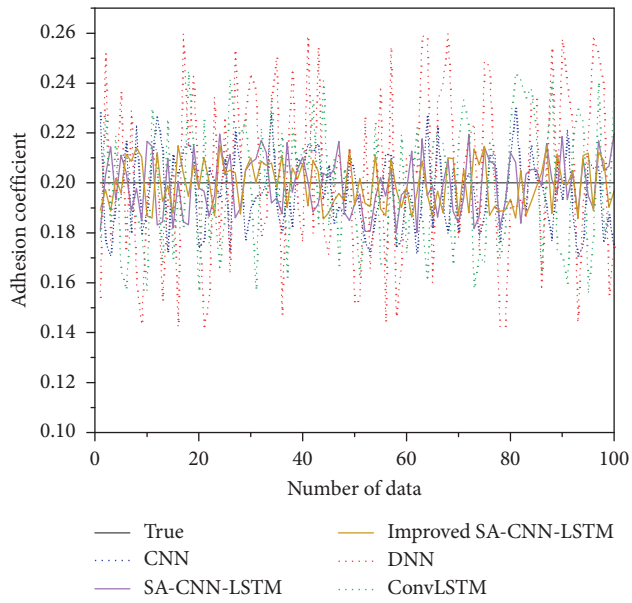

Figure 4: Comparison of prediction results under low adhesion coefficient.

Table 2: Comparison of prediction results under low adhesion coefficient.

Model	RMSE	MAE
DNN	0.034	0.029
CNN	0.017	0.015
ConvLSTM	0.025	0.021
SA-CNN-LSTM	0.012	0.010
Improved SA-CNN-LSTM	0.009	0.008

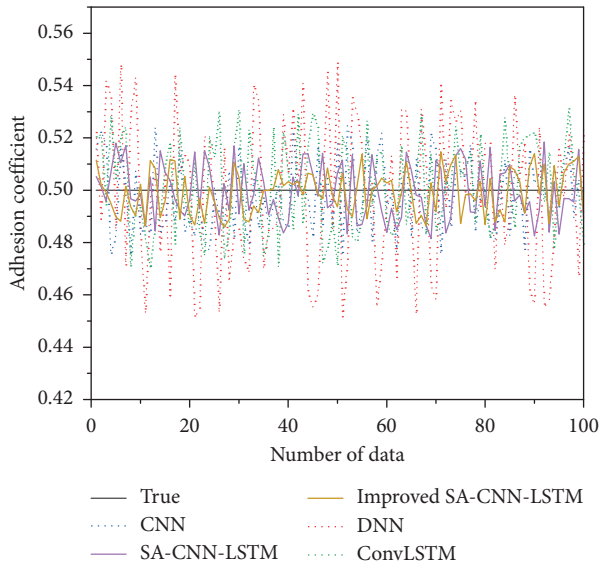

Figure 5: Comparison of prediction results under medium adhesion coefficient.

Table 3: Comparison of prediction results under medium adhesion coefficient.

Model	RMSE	MAE
DNN	0.029	0.025
CNN	0.014	0.012
ConvLSTM	0.018	0.016
SA-CNN-LSTM	0.010	0.009
Improved SA-CNN-LSTM	0.008	0.007

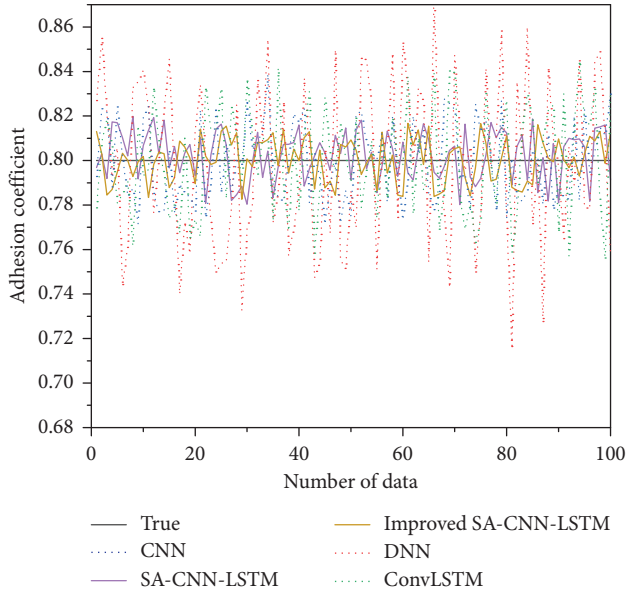

Figure 6: Comparison of prediction results under high adhesion coefficient.

Table 4: Comparison of prediction results under high adhesion coefficient.

Model	RMSE	MAE
DNN	0.037	0.031
CNN	0.018	0.016
ConvLSTM	0.026	0.012
SA-CNN-LSTM	0.013	0.010
Improved SA-CNN-LSTM	0.010	0.009

In the experiment, the adhesion coefficient of the dry road is estimated by the method proposed in this paper, while the transverse force coefficient of the wet road is obtained by the single-wheel transverse force test vehicle. Although the operating conditions are different, the two results are interrelated. First of all, the total tire adhesion is a vector, and the utilization effect is equivalent in the longitudinal or transverse direction. Secondly, there is a proportional relationship between the friction coefficient of the same road under dry and wet conditions. Average the results of the two methods in each test group and calculate the ratio of the mean values of the two methods to obtain Table 7.

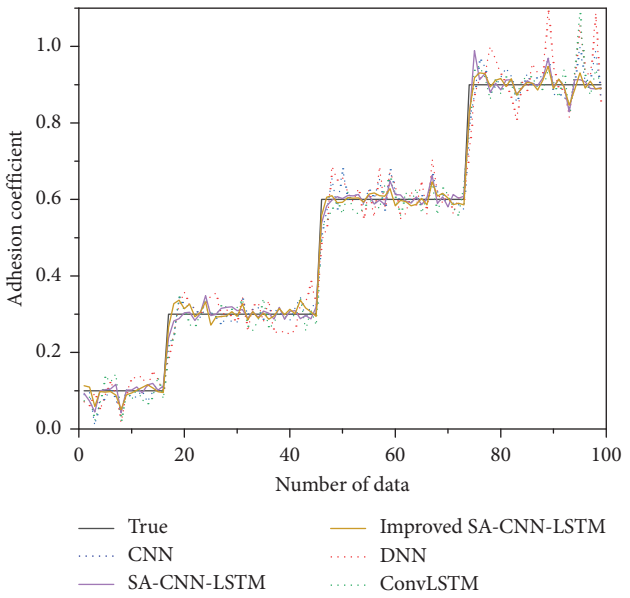

Figure 7: Comparison of prediction under the condition of increasing adhesion coefficient.

Table 5: Comparison of prediction under the condition of increasing adhesion coefficient.

Model	RMSE	MAE
DNN	0.048	0.035
CNN	0.026	0.018
ConvLSTM	0.029	0.023
SA-CNN-LSTM	0.021	0.014
Improved SA-CNN-LSTM	0.017	0.011

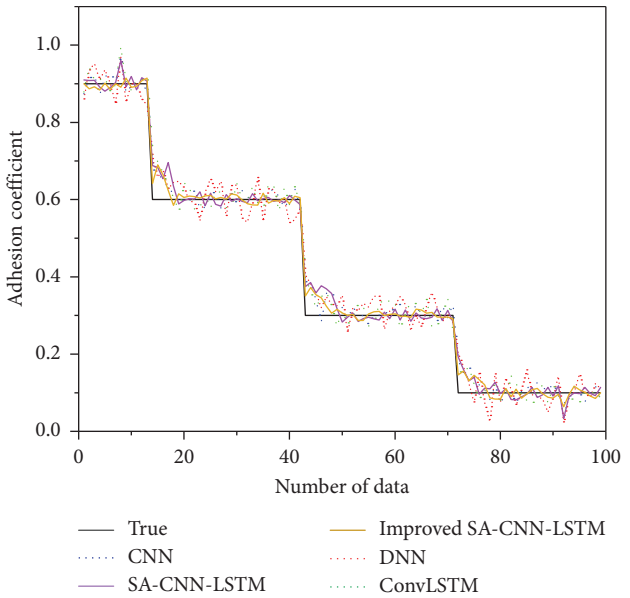

Figure 8: Comparison of prediction under the condition of decreasing adhesion coefficient.

Table 6: Comparison of prediction under the condition of decreasing adhesion coefficient.

Model	RMSE	MAE
DNN	0.040	0.033
CNN	0.025	0.019
ConvLSTM	0.031	0.027
SA-CNN-LSTM	0.023	0.015
Improved SA-CNN-LSTM	0.018	0.013

Table 7: Estimated results of the road adhesion coefficient.

Test group	Results of vehicle-based system	Results of single wheel transverse force test vehicle
First forward	0.628	0.408
Second forward	0.606	0.430
First reverse	0.576	0.426
Second reverse	0.616	0.431

It can be seen that the test results of the two methods are statistically stable under the same conditions. According to the Burckhardt tire-road model [33], the friction coefficient ratio of wet asphalt road and dry asphalt road is about 68%. The average friction coefficient of wet road obtained in this test is about 70% of that of dry road, which is basically consistent with the results of existing theories, indicating that the estimated value of this method is accurate.

6. Conclusion

Based on the CarSim simulation data and vehicle-based data of vehicle network cloud integration, this paper analyzes the vehicle operation data related to the road adhesion coefficient, constructs the SA-CNN-LSTM adhesion coefficient estimation model, and optimizes it with the reinforcement learning Q-learning algorithm, which has higher accuracy than DNN, CNN, and ConvLSTM. The specific conclusions are as follows:

(1) The road adhesion coefficient will affect the vehicle speed, acceleration, wheel angular velocity, and other parameters. The road adhesion coefficient can be estimated from these vehicle operation data.

(2) In terms of example verification using simulation data, under the five conditions of low adhesion coefficient, medium adhesion coefficient, high adhesion coefficient, increasing adhesion coefficient, and decreasing adhesion coefficient, compared with other models, SA-CNN-LSTM decreased by 29.41%, 25.57%, 27.78%, 19.23%, and 8% in RMSE and 33.3%, 25%, 25%, 22.2%, and 21.01% in Mae, respectively. Improved SA-CNN-LSTM can be further reduced by 25%, 20%, 23%, 23.8%, and 21.7% on RMSE, and 20%, 22.2%, 10%, 21.4%, and 13.3% on MAE.

(3) In terms of example verification using vehicle-based data, the ratio of the estimated results of road adhesion coefficient to the results of the standard method is basically consistent with the results of existing theories, which shows the accuracy of this method.

However, the work of this paper also has some shortcomings. In the future work, we will collect more data to verify the effectiveness of the model in a variety of different scenarios.

Data Availability

The raw data required to reproduce these findings cannot be shared at this time as the data also form part of an ongoing project and study.

Conflicts of Interest

The authors declare that they have no conflicts of interest.

Acknowledgments

This research was supported by the projects of Hebei Provincial Department of Transportation (grant no. RW-202007) and Hebei Provincial Department of Science and Technology (grant no. 20310801D).

References

[1] C. Liu, "Adhesion coefficient of automobile tire and road surface," *Journal of Central South University of Technology*, vol. 15, no. 1, pp. 210–214, 2008.

[2] I. Novikov and D. Lazarev, "Experimental installation for calculation of road adhesion coefficient of locked car wheel," *Transportation Research Procedia*, vol. 20, pp. 463–467, 2017.

[3] H. Guo, Z. Yin, D. Cao, H. Chen, and C. Lv, "A review of estimation for vehicle tire-road interactions toward automated driving," *IEEE Transactions on Systems, Man, and Cybernetics: Systems*, vol. 49, no. 1, pp. 14–30, 2019.

[4] M. Morii, H. Yasuo, T. Kashihara, T. Iwamoto, and M. Sugimoto, "Road surface condition detector using high peak power fiber laser," *IEEE Transactions on Industry Applications*, vol. 120, no. 10, pp. 1198–1204, 2000.

[5] J. Ko, S. Ko, I. S. Kim, D. Y. Hyun, and H. S. Kim, "Cooperative control for regenerative braking and friction braking to increase energy recovery without wheel lock," *International Journal of Automotive Technology*, vol. 15, no. 2, pp. 253–262, 2014.

[6] S. Hong, G. Erdogan, K. Hedrick, and F. Borrelli, "Tyre–road friction coefficient estimation based on tyre sensors and lateral tyre deflection: modelling, simulations and experiments," *Vehicle System Dynamics*, vol. 51, no. 5, pp. 627–647, 2013.

[7] J. P. Paulo and J. Coelho, "Identification of road types using bayesian analysis and neural networks," *International Journal of Acoustics and Vibration*, vol. 22, pp. 289–295, 2017.

[8] K. Enisz, I. Szalay, G. Kohlrusz, and D. Fodor, "Tyre-road friction coefficient estimation based on the discrete-time extended Kalman filter," *Proceedings of the Institution of Mechanical Engineers-Part D: Journal of Automobile Engineering*, vol. 229, no. 9, pp. 1158–1168, 2015.

[9] B. Ma, C. Lv, Y. Liu, M. Zheng, Y. Yang, and X. Ji, "Estimation of road adhesion coefficient based on tire aligning torque distribution," *Journal of Dynamic Systems, Measurement, and Control*, vol. 140, no. 5, Article ID 51010, 2018.

[10] Y. Peng, J. Chen, and Y. Ma, "Observer-based estimation of velocity and tire-road friction coefficient for vehicle control systems," *Nonlinear Dynamics*, vol. 96, no. 1, pp. 363–387, 2019.

[11] X. Ping, S. Cheng, W. Yue, Y. Du, X. Wang, and L. Li, "Adaptive estimations of tyre-road friction coefficient and body's sideslip angle based on strong tracking and interactive multiple model theories," *Proceedings of the Institution of Mechanical Engineers-Part D: Journal of Automobile Engineering*, vol. 234, no. 14, pp. 3224–3238, 2020.

[12] J. Hu, S. Rakheja, and Y. Zhang, "Real-time estimation of tire-road friction coefficient based on lateral vehicle dynamics," *Proceedings of the Institution of Mechanical Engineers-Part D: Journal of Automobile Engineering*, vol. 234, no. 10-11, pp. 2444–2457, 2020.

[13] L. Shao, C. Jin, A. Eichberger, and C. Lex, "Grid search based tire-road friction estimation," *IEEE Access*, vol. 8, pp. 81506–81525, 2020.

[14] H. Bi, W. Shang, Y. Chen, K. Yu, and W. Y. Ochieng, "An incentive based road traffic control mechanism for COVID-19 pandemic alike emergency preparedness and response," *IEEE Transactions on Intelligent Transportation Systems*, vol. 23, no. 12, pp. 25092–25105, 2022.

[15] Y. Gao, J. Zhao, Z. Qin, Y. Feng, Z. Yang, and B. Jia, "Traffic speed forecast in adjacent region between highway and urban expressway: based on MFD and GRU model," *Journal of Advanced Transportation*, vol. 2020, Article ID 8897325, 18 pages, 2020.

[16] Y. Sun, L. Xiong, Z. Yu, Y. Feng, and L. Ren, "Road adhesion coefficient estimation," *Applied Mechanics and Materials*, vol. 52–54, pp. 1503–1508, 2011.

[17] S. Li, X. Pei, Y. Ma, and L. Tao, "A new road friction coefficient estimation method based on SVM," in *Proceedings of the 2012 International Conference on Mechatronics and Automation (ICMA)*, pp. 1910–1914, Chengdu, China, August 2012.

[18] D. J. Kim, S. K. Jin, S. H. Lee, and C. C. Chung, "A comparative study of estimating road surface condition using support vector machine and deep neural network," in *Proceedings of the 2019 IEEE Intelligent Transportation Systems Conference (ITSC)*, pp. 1066–1071, Auckland, New Zealand, October 2019.

[19] A. M. Ribeiro, A. Moutinho, A. R. Fioravanti, and E. C. de Paiva, "Estimation of tire–road friction for road vehicles: a time delay neural network approach," *Journal of the Brazilian Society of Mechanical Sciences and Engineering*, vol. 42, no. 1, p. 4, 2020.

[20] M. Choi, J. J. Oh, and S. B. Choi, "Linearized recursive least squares methods for real-time identification of tire-road friction coefficient," *IEEE Transactions on Vehicular Technology*, vol. 62, no. 7, pp. 2906–2918, 2013.

[21] Š. Eldar, Ž. Vidas, O. Prentkovskis, and V. Skrickij, "Identification of road-surface type using deep neural networks for friction coefficient estimation," *Sensors*, vol. 20, 2020.

[22] R. He, E. Jimenez, D. Savitski, C. Sandu, and V. Ivanov, "Investigating the parameterization of dugoff tire model using experimental tire-ice data," *SAE International Journal of Passenger Cars-Mechanical Systems*, vol. 10, no. 1, pp. 83–92, 2016.

[23] C. Ren, C. Chai, C. Yin et al., "Short-term traffic flow prediction: a method of combined deep learnings," *Journal of Advanced Transportation*, vol. 2021, Article ID 9928073, 15 pages, 2021.

[24] J. Zhao, Z. Yu, X. Yang, Z. Gao, and W. Liu, "Short term traffic flow prediction of expressway service area based on STL-OMS," *Physica A: Statistical Mechanics and Its Applications*, vol. 595, Article ID 126937, 2022.

[25] Y. Qiao, Y. Wang, C. Ma, and J. Yang, "Short-term traffic flow prediction based on 1DCNN-LSTM neural network structure," *Modern Physics Letters B*, vol. 35, no. 2, 2021.

[26] D. Liu, L. Tang, G. Shen, and X. Han, "Traffic speed prediction: an attention-based method," *Sensors*, vol. 19, no. 18, p. 3836, 2019.

[27] A. Vaswani, N. Shazeer, N. Parmar et al., "Attention is all you need," 2017, https://arxiv.org/abs/1706.03762.

[28] Y. Wu, H. Tan, L. Qin, B. Ran, and Z. Jiang, "A hybrid deep learning based traffic flow prediction method and its understanding," *Transportation Research Part C: Emerging Technologies*, vol. 90, pp. 166–180, 2018.

[29] H. Yu, Z. Wu, S. Wang, Y. Wang, and X. Ma, "Spatiotemporal recurrent convolutional networks for traffic prediction in transportation networks," *Sensors*, vol. 17, no. 7, p. 1501, 2017.

[30] J. Zhao, Y. Gao, Z. Bai, H. Wang, and S. Lu, "Traffic speed prediction under non-recurrent congestion: based on LSTM method and BeiDou navigation satellite system data," *IEEE Intelligent Transportation Systems Magazine*, vol. 11, no. 2, pp. 70–81, 2019.

[31] W. Hao, D. Rong, K. Yi et al., "Traffic status prediction of arterial roads based on the deep recurrent Q-learning," *Journal of Advanced Transportation*, vol. 2020, Article ID 8831521, 17 pages, 2020.

[32] W. Shang, Y. Chen, X. Li, and W. Y. Ochieng, "Resilience analysis of urban road networks based on adaptive signal controls: day-to-day traffic dynamics with deep reinforcement learning," *Complexity*, vol. 2020, Article ID 8841317, 19 pages, 2020.

[33] M. Dousti, S. C. Baslamisli, E. T. Onder, and S. Solmaz, "Design of a multiple-model switching controller for ABS braking dynamics," *Transactions of the Institute of Measurement and Control*, vol. 37, no. 5, pp. 582–595, 2015.